D2.3 | Thermoelectric characterization

Author(s): Maria Spies, Elia Strambini

Delivery date: 24.06.2021
Version: 2.0

This project has received funding from the European Union's Horizon 2020 research and innovation programme under grant agreement No 800923.

Project Acronym:	SUPERTED
Project Full Title:	Thermoelectric detector based on superconductor-ferromagnet heterostructures
Call:	H2020-FETOPEN-2016-2017
Topic:	FETOPEN-01-2016-2017
Type of Action:	RIA
Grant Number:	800923
Project URL:	https://superted-project.eu/

Editor:	Maria Spies, CNR Pisa; Elia Strambini, CNR Pisa
Deliverable nature:	Report (R)
Dissemination level:	Public (PU)
Contractual Delivery Date:	28.02.2020
Actual Delivery Date :	25.02.2021 version 1.0 24.06.2021 version 2.0
Number of pages:	16
Keywords:	Superconducting thermoelectric detector, ferromagnetic insulator-superconductor heterostructures, tunneling spectroscopy, spin-splitting
Author(s):	Maria Spies, CNR Pisa Elia Strambini, CNR Pisa Pauli Virtanen, JYU Stefan Ilic, CSIC
Contributor(s):	Sara Khodishian, CNR Pisa Nadia Ligato, CNR Pisa Tero Heikkilä, JYU Sanna Rauhamäki, JYU
External contributor(s):	Jagadeesh Moodera, MIT, USA

Abstract

The deliverable 2.3 *'Thermoelectric characterization'* of Work Package 2 gives an overview over the experimental results obtained in the project period September 2019 – February 2021 relating to the thermoelectric behavior of ferromagnetic insulator (FI) and superconductor (S) bilayers. Tunneling spectroscopy has been carried out on such structures in order to investigate the influence of a thermal component on the behavior of the tunnel junction. The thermal gradient has been generated by Joule heating of the normal metal (N) leads. Interestingly, this heating configuration revealed not only the predicted thermovoltage[1] but also a giant rectification effect induced by the heating current. This rectification effect can find its application in a radiation detector and has therefore been investigated in more detail.

This project has received funding from the European Union's Horizon 2020 research and innovation programme under grant agreement No 800923.

The thermoelectric behavior of the N/FI/S structure has therefore subsequently been modelled in order to discern the components of the different phenomena: rectification and thermovoltage. Two measurement schemes have been explored in the spin-split ferromagnetic tunnel junctions. In the first one, conventional rectification was observed in the current vs voltage (IV) characteristics measured across the junction and due to the natural asymmetry generated by the spin splitting and filtering of the device. Rectification was considered and analyzed in both current and voltage bias. In the second scheme based on a transversal measurement, both rectification and thermovoltage were observed with a dominant contribution from rectification. A signal as large as 7 μV (21 μV) at a magnetic field of 0 T (0.1 T) has been observed for the rectification component. A temperature dependence of the differential conductance and the rectification voltage are shown and discussed.

This project has received funding from the European Union's Horizon 2020 research and innovation programme under grant agreement No 800923.

HISTORY OF CHANGES		
VERSION	DATE	CHANGE
1.0	25.02.2021	Initial version
2.0	24.06.2021	Addition of Chapter 3 Thermoelectricity before the chapter on Temperature dependence of rectification. The numbering of following chapters was adjusted accordingly. This chapter on Thermoelectricity was missing from the initial version due to an error in the submission process as a wrong version was submitted initially. Accordingly, the introduction, the end of chapter 2, discussing the figure 3 as well as the conclusions and outlook reflect the additions that were omitted in error from the initial submission.
2.0	24.06.2021	**1st suggestions for revision:** *It is not quantified the contribution of the thermovoltage deduced by theoretical simulations (not explained).* We have added a subchapter to the report outlining the theoretical considerations on the different contributitons of rectification and thermoelectricity. The contribution of the thermovoltage to the symmetric voltage has been quantified as a percentage (~20–40%). It is furthermore outlined that it has the opposite sign i.e. act as a compensation of the rectification. We have specified: ”At a heating current of 200 μA the symmetric voltage has a thermoelectric component of 5-10 μV in both experiment and theory which act opposing the rectification.” and ”Furthermore, we can extract from these simulations that the Seebeck coefficient S is of the order of 0.7 k_B/e, if V_{sym} is about 5 μV.”
2.0	24.06.2021	**2nd suggestion for revision:** *It is not clear if it is planned to use rectification as a tool for radiation detection or if a structure where the thermovoltage effect dominates is preferred.* In chapter 3 we added: ”Note that both rectification and thermoelectricity are always present in these structures. One cannot turn off one or the other. One can only optimize the structure in such a way that a dominance of one of the two is achieved.” and ”At this moment, a detector based on the thermoelectric effect as well as one based on rectification is conceivable. It is at this moment not clear if one would outperform the other. This is one of the central questions of our investigations going forward.”
2.0	24.06.2021	**3rd suggestion for revision:** *Some parts of the report are not accurate. For instance, two figure captions start with Figure 2, Figure 4 is not numbered in the caption, but is mentioned in the main text.* The incorrect labeling and remaining typos have been corrected.

This project has received funding from the European Union’s Horizon 2020 research and innovation programme under grant agreement No 800923.

1. Introduction

The central building block of the superconducting thermoelectric detector of the EU Horizon 2020-funded SuperTED project is the quantification of the thermoelectric component of the spin-split ferromagnetic tunnel junctions[2] used in said detectors. A giant thermoelectricity has been predicted[1] for such ultra-sensitive radiation detectors[3]. These detectors are "self-powered" thanks to the incoming radiation, i.e., the detector signal arises from absorbed radiation, and no bias is needed. They are hence different from the presently pursued concepts of transition edge sensors[4,5] and kinetic inductance detectors[6], that require a bias for their read-out. The lack of a bias line simplifies the construction of the detector, allows for bigger detector arrays and allows getting rid of the bias-induced heating that has an adverse effect on the detector resolution.

In the Deliverable 2.3 of the SuperTED project we investigated and quantified the thermoelectric properties of the best Cu/EuS/Al junctions provided by the MIT subcontractor which were pre-characterized in the previous Deliverables 2.1 and 2.2. Interestingly, this characterization led us to discover that the heating current injected to simulate the absorption of radiation generates not only a thermoelectric signal but also a strong rectification. Rectification and thermoelectricity are two inseparable phenomena originating from electron-hole asymmetric transport, but such a strong rectification signal was not considered in the first theoretical attempts. Through a proper design of the sample geometry, however, it is possible to enhance one aspect with respect to the other and avoid negative competing effects.

In the first part of this Deliverable report we present results on the conventional rectification of the ferromagnetic tunnel junction. It is considered for both current and voltage bias.

In the second part we present results on the transversal rectification of the spin-split ferromagnetic tunnel junction. This setup was primarily used to study the thermoelectric effect, which requires a temperature difference across the thermoelectric junction. In the thermoelectric detector this temperature difference would be generated by the external radiation absorbed in one part of the device. This temperature difference then produces the thermoelectric current or voltage across the junction. Here we mimic the effect of this external radiation by applying a heating current to the normal part (Cu) of the device. As expected, we found a sizable transverse voltage across the N-FI-S junction produced by this heating current. However, a closer analysis of this transverse voltage revealed that its main origin was the rectification. The contribution of a thermovoltage can be deduced from the theoretical simulations but remains dominated by that of the rectification. A temperature dependence of the differential conductance and the rectification voltage are shown and discussed.

A conclusion and outlook with suggestions for further research is given in the last part.

All tunneling spectroscopy measurements are carried out at cryogenic temperatures, at 25 mK, in a filtered cryogen-free dilution refrigerator with typical RC filter resistances of around 2 kΩ at NEST labs at CNR-Nano in Pisa, Italy. The V−I characteristics are obtained from a DC four-wire measurement. It is used to calculate the differential conductance via numerical differentiation.

The samples were provided through the collaboration with Dr. J. S. Moodera at MIT, Boston, MA, USA. The samples are cross-bars made by electron-beam evaporation employing an in-situ

This project has received funding from the European Union's Horizon 2020 research and innovation programme under grant agreement No 800923.

shadow mask. The structures consist of a glass substrate on which the layers of Cu/ EuS/ Al are deposited subsequently. The area of the overlap of the Al and the Cu strip is around 300×300 m^2.

This project has received funding from the European Union's Horizon 2020 research and innovation programme under grant agreement No 800923.

2. Rectification

Normal metal – ferromagnetic insulator – superconductor (N/FI/S) tunnel junctions are investigated. The N component is a Cu strip which crosses the S component, an Al strip, at a right angle. Between the two, the FI EuS constitutes the spin-polarized barrier. Two measurement configurations have been compared. In the first one (I) a current is applied from the N to the S, effectively crossing the junction and conventional rectification is observed. In the other one (II) a current is applied along the N strip and a transversal rectification is observed, i.e a voltage signal orthogonal to the current path. In both cases the voltage drop is measured from the N to the S across the tunnel junction. Measurements of the two configurations are compared and discussed below.

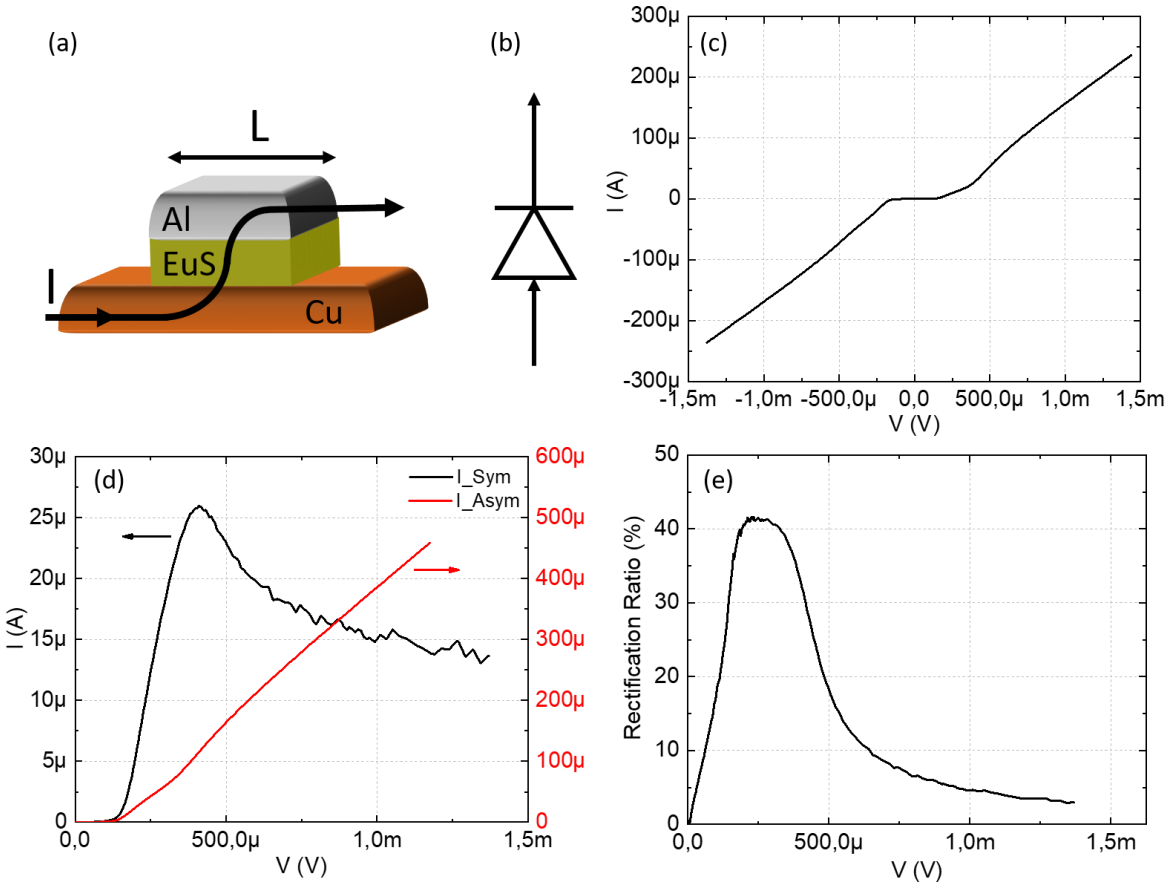

Figure 1. Measuring the conventional rectification of the ferromagnetic tunnel junction in voltage bias. (a) Schematic of the N/FI/S tunnel junction. The path of the tunneling current is indicated by the black line and its arrows. (b) Electronic circuit diagram of the setup. (c) I-V characteristics of the measurement setup sketched in (a). (d) Symmetric and asymmetric parts of the I-V characteristics and (e) the rectification ratio which is the highest, (41 %), around 225 – 280 V.

Conventional rectification

A typical tunnel junction with conventional rectification can be seen in Figure 1. It corresponds to measurement configuration (I) in voltage bias. The current bias is considered below in Figure 2. In

This project has received funding from the European Union's Horizon 2020 research and innovation programme under grant agreement No 800923.

either case the voltage (current) bias and the output current (voltage) are measured across the junction. The effect of the superconducting gap can be clearly seen in the I-V characteristic given in Figure 1(c) with a plateau of no current flow around 0 V and the Ohmic (linear) behavior for relatively large voltages. The symmetric and asymmetric parts of the IV characteristics have been calculated in order to quantify the junction's rectification. They are defined as

$$I_{Sym} = \frac{I(V) + I(-V)}{2}$$

$$I_{Asym} = \frac{I(V) - I(-V)}{2}$$

where the same operations can be carried out for both the symmetric and asymmetric parts of the voltage using the current.

Both calculated components of the current as a function of voltage are given in Figure 1(d). The sizable $I_{Sym}(V)$ already demonstrates the efficient rectification to convert an AC input in to DC output signals. The DC rectified signal, if the junction were operated with an AC current, corresponds to the symmetric part.

The rectification R of a circuit can be defined as the ratio between the difference of the forward and backward flow divided by the sum of the two $R= (I_f - I_b)/(I_f + I_b)$. For ideal rectifiers R=1 while for R=0 no rectification is present.

From the symmetric and asymmetric parts of the I-V characteristics it is possible to calculate the rectification defined as $R = I_{Sym}/I_{Asym}$ and given in (e) as a function of the voltage bias. Thanks to the strong asymmetry induced by the spin filtering for this specific junction the R is the highest around 225 - 280 μV where it reaches 41% rectification. The same analysis can be fulfilled in the current bias configuration as reported in Fig 2 in which the rectification is defined as $R = V_{Sym}/V_{Asym}$.

This project has received funding from the European Union's Horizon 2020 research and innovation programme under grant agreement No 800923.

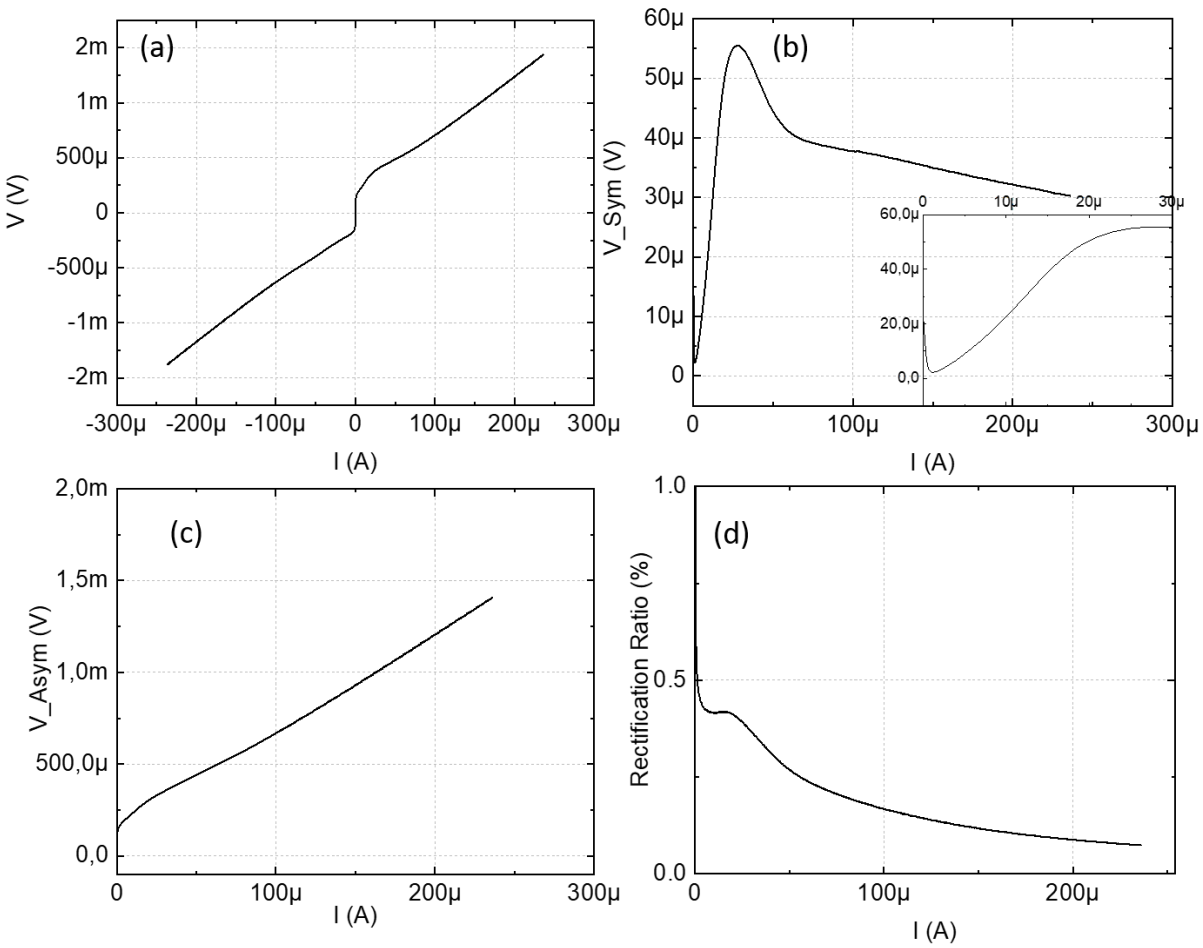

Figure 2. (a) V-I characteristics of the measurement setup sketched in Fig 1(a). (b) Symmetric part of V-I characteristics, inset: zoomed to 0-30 uA, (c) the asymmetric part and (d) the rectification ratio.

Transversal rectification

In Figure 3 we show the same tunnel junction which is measured, however, in a way that a transversal rectification occurs. This corresponds to measurement configuration (II). The current is applied along the N strip rather than across the junction while the voltage drop is again measured across the junction. The device is operated in current bias and the output voltage is measured for different applied magnetic fields. At the tunnel junction the current is split in two paths, one along the N lead and one through the EuS to the S lead and back to the N. Thanks to the rectification properities shown in Fig. 2, the latter can generate a voltage drop across the junction proportional to the current and R. This is shown in Fig. 3c for different applied magnetic fields B.

With increasing applied magnetic field the output voltage approaches a linear behavior. Interestingly, thanks to the ferromagnetic aspect of the FI layer, the structure can be operated even at no applied magnetic field while maintaining a reasonable output signal (see black data in panel (c)). This is especially relevant for applications as no additional components are needed to be integrated into a device for the generation of an external magnetic field and no additional power supply is

This project has received funding from the European Union's Horizon 2020 research and innovation programme under grant agreement No 800923.

necessary. Furthermore, the impedance of the configuration (II) is lower than that of configuration (I). That makes it more suitable for the use as a radiation detector compared to measurement configuration (I) because it allows separately tuning the contact impedance determining the size of the signal and the radiation absorber resistance for optimized quantum efficiency, i.e., optimized amount of absorbed radiation into the device.

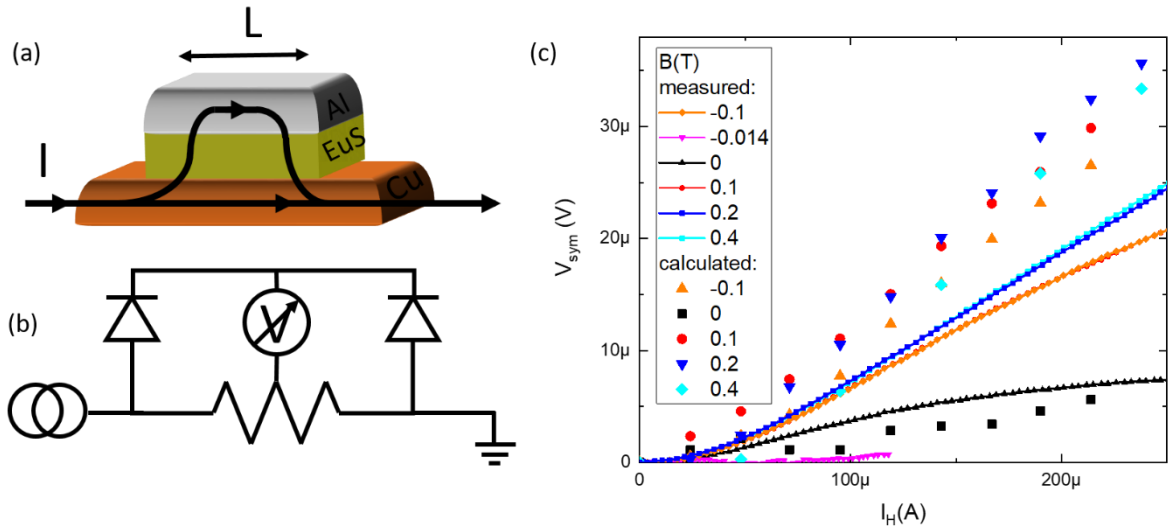

Figure 3. Measuring the transversal rectification of a spin-split tunnel junction.(a) Schematic of the N/FI/S tunnel junction and the current flow. A heating current is applied from one end of the Cu strip to the other, while the voltage drop across the junction is measured. The path of the tunneling current indicated by the black lines and its arrows. (b) Electronic circuit diagram of the setup. Note that the EuS layer effectively acts as a rectifying component. (c) V-I characteristics of the measurement setup sketched in (a) for different values of the magnetic field. Note that even at no applied magnetic field (black curve) a voltage drop occurs as a consequence of the permanent magnetization of the EuS. The V-I was symmetrized in order to discard the Ohmic (linear) component originating from the N lead. The calculated data points were obtained by means of a theoretical model of the circuit and using the rectification value obtained from the experimentally measured data in Fig. 2.

In Fig. 3(c), we calculate the rectification voltage at different heating currents I_H from the experimentally measured I-V curves using the following theoretical model. The open circuit voltage V_s for the configuration shown in Fig. 3 (a) can be determined by solving the equation

$$\int_0^1 I(s\, I_H R_x + V_s + V_{inst}) ds = 0.$$

Here R_x is the lateral resistance of the junction, and V_{inst} is the instrumental offset. V_s containts two contributions: the larger trivial part due to the heating current, and a smaller part due to rectification.

This project has received funding from the European Union's Horizon 2020 research and innovation programme under grant agreement No 800923.

The former is antisymmetric in I_H, whereas the latter is symmetric. Therefore, the symmetrized voltage

$$V_{th} = \frac{1}{2}[V_s(I_H) + V_s(-I_H)]$$

comes from rectification effect only. As seen on Fig. 3(c), our theoretical calculations are generally larger than measured data by about 30%. This difference likely comes from the thermoelectric effect, which produces thermovoltage of the opposite sign to the rectification voltage.

This project has received funding from the European Union's Horizon 2020 research and innovation programme under grant agreement No 800923.

3. Thermoelectricity

The measured symmetric component of the voltage contains contributions from both rectification and thermoelectricity. Which one is more important is not universal, but depends on the electrical and thermal parameters and sample geometry. In particular, the transversal length of the cross junction (i.e the width of the S lead) determines the voltage drop driving the rectification. Note that both rectification and thermoelectricity are always present in these structures. One cannot turn off one or the other. One can only optimize the structure in such a way that a clear dominance of one of the two is achieved. Based on thermal modeling, we estimate that thermoelectricity dominates when the junction width is below a cross-over length

$$L_c = \sqrt{\frac{2t_{\mathrm{Al}}\rho_{\square,\mathrm{tun}}\Sigma_{\mathrm{Al}}}{\rho_{\mathrm{Cu}}\Sigma_{\mathrm{Cu}}}} \approx 100\,\mu\mathrm{m}$$

which depends on the aluminum layer thickness (t_{Al}), copper and tunnel junction (square) resistivities(ρ_{Cu} and $\rho_{\square,\mathrm{tun}}$), and the electron-phonon coupling constants for Copper and Aluminum (Σ_{Cu} and Σ_{Al}).

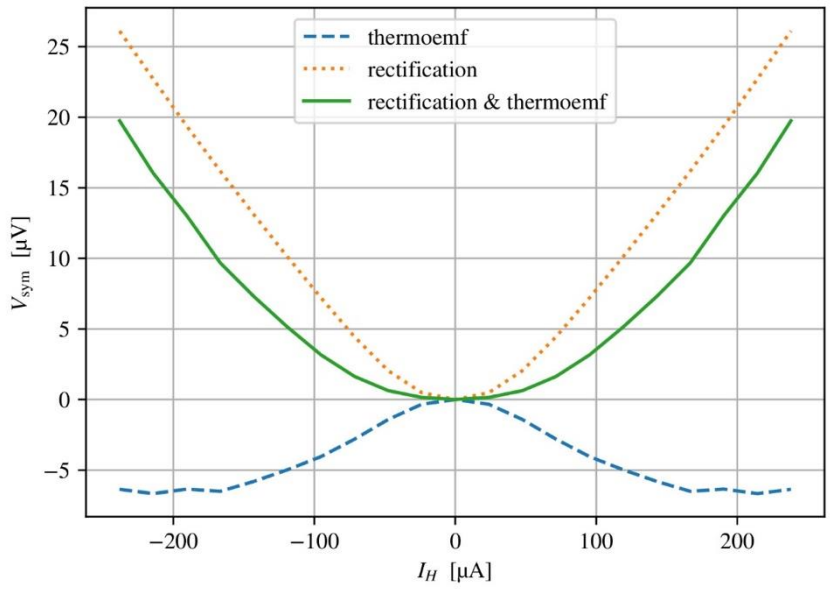

Figure 4. Comparison of predicted thermoelectric and rectification voltages. The theoretical prediction is based on temperatures extracted from the experimental data with a thermal model, and fitted junction parameters at B=0.2 T.

In the experiment discussed above, the junction width is ~ 280μm, and rectification hence dominates. We have quantified the effect with a thermal model fitted to the experimental results, with results shown in Figure 4. Due to the weaker electron-phonon coupling in the superconductor ($\Sigma_{\mathrm{Al}} \ll$

This project has received funding from the European Union's Horizon 2020 research and innovation programme under grant agreement No 800923.

Σ_{Cu}), and the fact that a part of the current tunnels into it, the superconductor temperature is higher than that on the normal side. As a consequence, the thermoelectric voltage has the opposite sign as compared to rectification voltage which means it compensates it. Its magnitude is predicted to be ~20–40% of the rectification voltage. The magnitude of the symmetric voltage in the model is in a reasonable agreement with what is seen in the experiment. At a heating current of 200 μA the symmetric voltage has a thermoelectric component of 5-10 μV in both experiment and theory which act opposing the rectification. Furthermore, we can extract from these simulations that the Seebeck coefficient S is of the order of 0.7 k_B/e, if V_{sym} is about 5 μV.

At this moment, a detector based on the thermoelectric effect as well as one based on rectification is conceivable. It is at this moment not clear if one would outperform the other. This is one of the central questions of our investigations going forward.

This project has received funding from the European Union's Horizon 2020 research and innovation programme under grant agreement No 800923.

4. Temperature dependence of rectification

In Figure 5 we show the temperature dependence of the differential conductance and the rectification voltage of the discussed tunnel junction. Increasing the temperature will lower the asymmetry of the IV characteristic via thermal broadening and as a consequence the rectification. Interestingly, the tunnel junction shows clear responsivity up 1.7 K, i.e., to a temperature higher than one half of the critical temperature T_c of superconductivity in Al without much degradation due to thermal averaging. This behavior is expected to hold for other superconductor materials and can be extended to higher temperatures. The advantage of an electromagnetic radiation sensor based on the device design and measurement configuration presented here is therefore that it can be operated at standard He4 cryogenic temperatures.

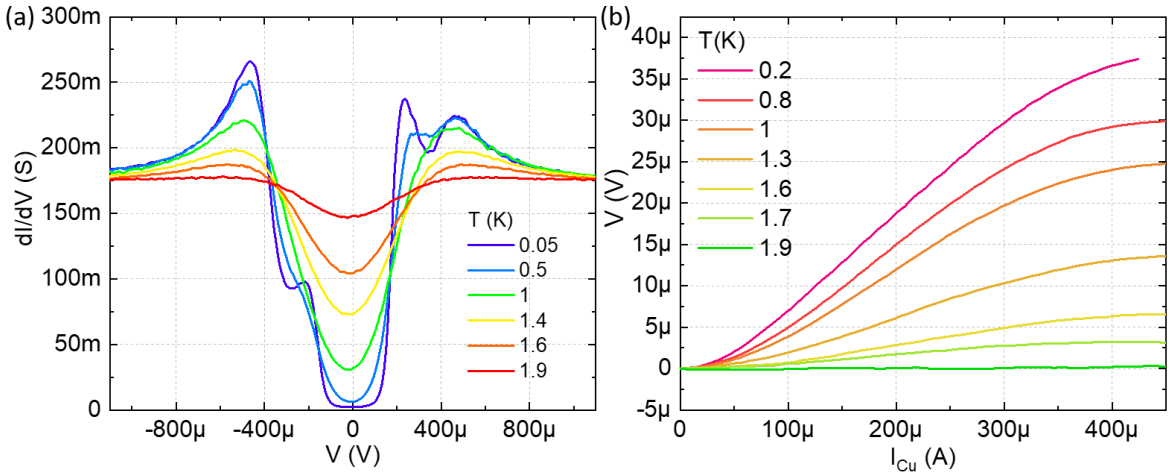

Figure 5. Temperature dependence up to 1.9 K. (a) the differential conductance vs V and (b) the rectification voltage vs the heating current in the normal lead.

This project has received funding from the European Union's Horizon 2020 research and innovation programme under grant agreement No 800923.

5. Conclusion and Outlook

In conclusion, we have shown the capabilities of a N/FI/S tunnel junction to function as both a conventional and a transversal rectifier. Considerations on the thermovoltage for the transversal rectifier have been presented and its contribution were found to be lower but of the same size compared to the rectification itself. The transversal rectifier benefits from a lower impedance and can be operated without external applied magnetic field. It is a promising step towards the development of detectors in the THz region contributing to terahertz gap closure.

From the modeling and fitting of the experimental data we understood that rectification is favorable compared to thermoelectricity when the transversal length of the tunnel junction is longer than tens of micrometers. In order to design a structure preferring the effect of the thermovoltage over the rectification two alternative approaches can be explored in the future. One is based on the miniaturization of the junction to have shorter tunnel barriers. The other consists of the decoupling between the heater and the device lead through the addition of an external heating component in the shape of a meander which externally heats the junction through Joule heating while being electrically isolated from the rest of the device. In that way the rectification cannot occur and observed effects will stem solely from the heat of the external resistance. Still, the optimal design of the final detector requires the antenna to be in good electrical contact to one of the leads, therefore rectification cannot be neglected and will need to be properly accounted. In particular, the rectified voltage has the same sign as that produced by heating the normal side. This should then be taken into account when planning the heat balance related with the radiation detection.

This project has received funding from the European Union's Horizon 2020 research and innovation programme under grant agreement No 800923.

Bibliography

(1) Ozaeta, A.; Virtanen, P.; Bergeret, F. S.; Heikkilä, T. T. Predicted Very Large Thermoelectric Effect in Ferromagnet-Superconductor Junctions in the Presence of a Spin-Splitting Magnetic Field. *Phys. Rev. Lett.* **2014**, *112* (5), 057001. https://doi.org/10.1103/PhysRevLett.112.057001.

(2) Meservey, R.; Tedrow, P. M. Spin-Polarized Electron Tunneling. *Phys. Rep.* **1994**, *238* (4), 173–243. https://doi.org/10.1016/0370-1573(94)90105-8.

(3) Heikkilä, T. T.; Ojajärvi, R.; Maasilta, I. J.; Strambini, E.; Giazotto, F.; Bergeret, F. S. Thermoelectric Radiation Detector Based on Superconductor-Ferromagnet Systems. *Phys. Rev. Appl.* **2018**, *10* (3), 034053. https://doi.org/10.1103/PhysRevApplied.10.034053.

(4) Irwin, K. D.; Hilton, G. C. Transition-Edge Sensors. In *Cryogenic Particle Detection*; Enss, C., Ed.; Ascheron, C. E., Kölsch, H. J., Skolaut, W., Series Eds.; Topics in Applied Physics; Springer Berlin Heidelberg: Berlin, Heidelberg, 2005; Vol. 99, pp 63–150. https://doi.org/10.1007/10933596_3.

(5) Ullom, J. N.; Bennett, D. A. Review of Superconducting Transition-Edge Sensors for x-Ray and Gamma-Ray Spectroscopy. *Supercond. Sci. Technol.* **2015**, *28* (8), 084003. https://doi.org/10.1088/0953-2048/28/8/084003.

(6) Baselmans, J. Kinetic Inductance Detectors. *J. Low Temp. Phys.* **2012**, *167* (3–4), 292–304. https://doi.org/10.1007/s10909-011-0448-8.

(7) Baliga, B. J. *Fundamentals of Power Semiconductor Devices*; Springer International Publishing: Cham, 2019. https://doi.org/10.1007/978-3-319-93988-9.

This project has received funding from the European Union's Horizon 2020 research and innovation programme under grant agreement No 800923.